THE JOURNAL OF BIOLOGICAL CHEMISTRY
Vol. 278, No. 31, Issue of August 1, pp. 28831–28839, 2003

Printed in U.S.A.

Antifungal Activity of Amiodarone Is Mediated by Disruption of Calcium Homeostasis*

Received for publication, March 31, 2003, and in revised form, May 7, 2003
Published, JBC Papers in Press, May 16, 2003, DOI 10.1074/jbc.M303300200

Soma Sen Gupta‡§¶, Van-Khue Ton‡¶, Veronica Beaudry‖, Samuel Rulli‡, Kyle Cunningham‖, and Rajini Rao‡

From the Departments of ‡Physiology and ‖Biology, The Johns Hopkins University, Baltimore, Maryland 21205

The antiarrhythmic drug amiodarone was recently demonstrated to have novel broad range fungicidal activity. We provide evidence that amiodarone toxicity is mediated by disruption of Ca^{2+} homeostasis in *Saccharomyces cerevisiae*. In mutants lacking calcineurin and various Ca^{2+} transporters, including pumps (Pmr1 and Pmc1), channels (Cch1/Mid1 and Yvc1), and exchangers (Vcx1), amiodarone sensitivity correlates with cytoplasmic calcium overload. Measurements of cytosolic Ca^{2+} by aequorin luminescence demonstrate a biphasic response to amiodarone. An immediate and extensive calcium influx was observed that was dose-dependent and correlated with drug sensitivity. The second phase consisted of a sustained release of calcium from the vacuole via the calcium channel Yvc1 and was independent of extracellular Ca^{2+} entry. To uncover additional cellular pathways involved in amiodarone sensitivity, we conducted a genome-wide screen of nearly 5000 single-gene yeast deletion mutants. 36 yeast strains with amiodarone hypersensitivity were identified, including mutants in transporters (*pmr1*, *pdr5*, and vacuolar H^+-ATPase), ergosterol biosynthesis (*erg3*, *erg6*, and *erg24*), intracellular trafficking (*vps45* and *rcy1*), and signaling (*ypk1* and *ptc1*). Of three mutants examined (*vps45*, *vma3*, and *rcy1*), all were found to have defective calcium homeostasis, supporting a correlation with amiodarone hypersensitivity. We show that low doses of amiodarone and an azole (miconazole, fluconazole) are strongly synergistic and exhibit potent fungicidal effects in combination. Our findings point to the potentially effective application of amiodarone as a novel antimycotic, particularly in combination with conventional antifungals.

The emergence of drug-resistant fungi poses an increasing threat to the treatment of opportunistic fungal infections in patients with compromised immune systems, as occurs commonly in cancer and AIDS. This can only be countered by the discovery of new antifungal agents, particularly those that target different molecular pathways, and a better understanding of their mode of action. Recently, the antiarrhythmic drug amiodarone (AMD)[1] was shown to have potent fungicidal activity against not only *Saccharomyces* but also pathogenic yeasts such as *Candida*, *Cryptococcus*, *Fusarium*, and *Aspergillus* (1). Viability of *Cryptococcus neoformans* after exposure to 10 μM AMD fell dramatically, with a 10-fold loss of viable cells after 1 h of treatment and only 0.001% viable cells remaining after 1 day. The cytotoxic effect of AMD appeared to be mediated by calcium, as evidenced by the ability of high (millimolar) concentrations of extracellular Ca^{2+} to ameliorate drug toxicity (1) and by an increase in cytosolic Ca^{2+} upon drug application (2).

There is emerging evidence that cytosolic Ca^{2+} entry in yeast is critical for survival under a variety of cell stresses, including hyper- and hypo-osmotic shock, protein unfolding agents, and antifungal drugs (3–6). The release of calcium from intracellular stores must be compensated by stimulation of extracellular calcium influx, a phenomenon commonly known as capacitative calcium entry (7). Thus, one possibility is that the cytosolic Ca^{2+} increase in response to AMD promotes cell survival and is due to capacitative calcium entry, as has been suggested by Courchesne and Ozturk (2). Paradoxically, excessive or unregulated levels of calcium in the cytoplasm also lead to cell death and are implicated in the cytotoxicity of several drugs (8) as well as fungal toxins (9, 10). To better understand the role of calcium in AMD toxicity, it is important to distinguish between a capacitative calcium entry mechanism triggered by store depletion or a loss in calcium homeostasis, possibly due to an effect of the drug on ion channels and transporters. The experiments described in this work address these two possibilities and begin to elucidate the cellular basis of AMD toxicity.

We present a detailed investigation of how AMD disrupts Ca^{2+} homeostasis in *Saccharomyces cerevisiae*. The roles of different Ca^{2+} transporters, including pumps (Pmr1 and Pmc1), channels (Cch1, Mid1, and Yvc1), and exchangers (Vcx1), were evaluated in cells lacking these proteins and exposed to relatively low, therapeutically relevant levels of AMD. Pmr1 is an ATP-driven pump that sequesters Ca^{2+} and Mn^{2+} into the Golgi/secretory pathway and maintains cellular ion homeostasis under normal growing conditions (11, 12). Homologues of Pmr1 are widely distributed in organisms including *Caenorhabditis elegans*, *Drosophila*, and humans and constitute the newly recognized SPCA subtype of Ca^{2+}-ATPases (13). Pmc1 is the yeast Ca^{2+} pump related to mammalian plasma membrane Ca^{2+}-ATPases that is induced under calcium stress (14) or in the absence of Pmr1 (12) and serves to detoxify excess

* This work was funded by a Burroughs Wellcome Student Elective Prize (to S. S. G.) and by National Institutes of Health Grant GM62142 and a grant-in-aid from the American Heart Association Mid-Atlantic Affiliate (to R. R.). The costs of publication of this article were defrayed in part by the payment of page charges. This article must therefore be hereby marked "*advertisement*" in accordance with 18 U.S.C. Section 1734 solely to indicate this fact.

§ Present address: Lucy Cavendish College, University of Cambridge, Cambridge CB3 OBU, United Kingdom.

¶ These authors contributed equally to this work.

** To whom correspondence should be addressed: Dept. of Physiology, The Johns Hopkins University School of Medicine, 725 N. Wolfe St., Baltimore, MD 21205. Tel.: 410-955-4732; Fax: 410-955-0461; E-mail: rrao@jhmi.edu.

[1] The abbreviations used are: AMD, amiodarone; BAPTA, 1,2-bis(2-aminophenoxy)-ethane-*N*,*N*,*N*′,*N*′-tetracetic acid; FLUC, fluconazole; MIC, miconazole; RLU, relative luminescence unit(s); WT, wild type; SC, synthetic complete.

Ca^{2+} by sequestration into the vacuole. Vacuolar calcium sequestration is also accomplished by the H^+/Ca^{2+} exchanger, Vcx1 (15–17), which requires the proton electrochemical gradient generated by the vacuolar H^+-ATPase. Calcium release from the vacuole is mediated by Yvc1, a transient receptor potential-like Ca^{2+} channel (18). Cch1 is the yeast homologue of mammalian voltage-gated calcium channels and, together with the stretch-activated Ca^{2+} channel Mid1, constitutes a Ca^{2+} entry channel at the plasma membrane (19). There is experimental evidence for at least one other calcium influx channel of unknown molecular identity (5, 20). Together, these proteins regulate cellular calcium levels and are critical for proper functioning of the calcium signaling cascade. Calcium activation of calmodulin and the consequent activation of the calcium- and calmodulin-activated protein phosphatase, calcineurin, are believed to lead to a number of transcriptional and post-translational signals that mediate a variety of different cellular responses to extracellular cues, including cell cycle progression and the protein kinase C-mediated cell wall integrity pathway (reviewed in Refs. 21 and 22). The conservation of several components of the calcium homeostatic machinery with higher eukaryotes makes yeast an excellent model to study the role of calcium signaling in AMD toxicity.

The results of our analysis of deletion mutants point to a requirement for Pmr1-mediated Ca^{2+} homeostasis in the growth response to AMD. Similar to recent observations on other drug resistance mechanisms (3, 6), we also demonstrate a critical role for calcineurin in AMD tolerance. Analyses of cytoplasmic Ca^{2+} levels by aequorin luminescence assays indicate a correlation between AMD-induced cytosolic Ca^{2+} increase and growth toxicity. Specifically, AMD seems to cause both Ca^{2+} influx at the cell membrane and release from internal stores, including the vacuole. To identify additional factors that mediate drug sensitivity, we screened nearly 5000 single-gene deletion mutants for hypersensitivity to AMD. We identify 36 mutants, implicated in known and novel pathways that may be important for drug resistance and detoxification. The results of this study indicate that AMD kills yeast by a mechanism different from that used by conventional antifungals such as the azoles and the polyenes. Finally, we show that low concentrations of AMD and an azole (miconazole and fluconazole) are strikingly synergistic in combination, suggesting that supplementation of conventional antifungal treatment with AMD may be a practical means of converting the fungistatic effect of the azoles into more effective fungicides. In summary, our findings provide important insights into the cellular effects of AMD and its potential efficacy in the treatment of fungal infections.

EXPERIMENTAL PROCEDURES

Yeast Strains and Media—Isogenic sets of yeast deletions were all derived from W303 and have been described before (15). The MATα *S. cerevisiae* deletion library was purchased from Research Genetics (Invitrogen). The Q783A and D53A mutations of PMR1 have been described (23, 24). *Candida albicans* SC5314 (25) was obtained from the laboratory of Brendan Cormack at The Johns Hopkins University School of Medicine, and *C. neoformans* (JEC21) (26) was a gift from the laboratory of Joseph Heitman at Duke University Medical Center. All yeast strains were grown in synthetic complete (SC) medium (Bio 101, Inc., Vista, CA) or standard YPD medium (2% Difco yeast extract, 1% bacto-peptone, 2% dextrose) at 30 or 37 °C as specified in the legends to Figs. 1, 5, and 6.

Growth Assays for Drug Sensitivity—AMD was purchased from Sigma, dissolved in dimethyl sulfoxide as a 20 mM stock, and stored at −20 °C. 10 μl of saturated seed cultures were inoculated in 3 ml of growth medium containing different concentrations of AMD (0–15 μM). Cultures were grown in a 30 °C shaker for 24 h, and growth was determined by optical density at 600 nm. To test the effect of divalent cations, AMD sensitivity was monitored in the presence of 10–25 mM $CaCl_2$ or 10 mM $MgCl_2$. Alternatively, the cation chelator 1,2-bis(2-aminophenoxy)-ethane-*N*,*N*,*N*′,*N*′-tetracetic acid (BAPTA; Sigma) was added to final concentrations of 0.5 and 2 mM. To examine the role of calcineurin inhibition, FK506 was diluted from a stock of 0.2 mg/ml to a final concentration of 1 μg/ml and added to cell cultures grown in stationary 96-well plates at 30 °C.

Miconazole and fluconazole were diluted from a stock of 5 mM (in Me_2SO) or 2 mg/ml (in water), respectively. In the fluconazole screen with *C. albicans*, the seed culture was diluted by 1:100 and added to 1 ml of YPD containing different drug concentrations in a 24-well plate. After a 24–48-h incubation at 37 °C, 5 μl of cells were diluted into 1.5 ml of YPD containing no drugs and grown overnight. Growth was measured by absorbance at 600 nM. With *C. neoformans*, 50 μl of saturated seed culture was added to 5 ml of YPD supplemented with various drug concentrations. Cells were shaken vigorously for 20 h at 30 °C. 5 μl of cells exposed to AMD alone or 20 μl of cells exposed to both drugs were then diluted in 10 ml YPD and grown to saturation for 24–48 h. Growth was measured by absorbance at 600 nM.

Genome-wide AMD Sensitivity Screen—200 μl of SC medium supplemented with 7 μM AMD was added to a 96-well plate and inoculated with 5 μl of freshly grown stationary phase yeast culture derived from single-gene deletion strains from the ResGen MATα deletion library (Invitrogen). Control cultures contained an equal volume of dimethyl sulfoxide. The plates were incubated at room temperature for a period of 12–24 h. Cultures were resuspended with a multichannel pipettor, and growth was monitored by measuring the absorbance at 600 nm in a SPECTRAmax 340 microplate reader (Molecular Devices). The relative growth of each strain was expressed as a percentage of A_{600} of the control culture (*i.e.* no AMD). Strains with enhanced sensitivity to AMD were selected based on growth inhibition of 80% or greater relative to control. All candidate strains were retested for enhanced sensitivity in 4 and 8 μM AMD.

Aequorin Luminescence Assay—Yeast strains were transformed with plasmid pEVP11-Aeq-89 (4) carrying the aequorin gene and then grown to midlog phase in SC medium lacking leucine. Cells were harvested, incubated with 0.25 mg/ml coelenterazine (Molecular Probes, Inc., Eugene, OR) in the dark for 20 min, washed and resuspended in medium, and then incubated at 30 °C for 90 min to allow recovery. AMD (at specified concentrations) was added to 0.3 ml of cells in a cuvette through an injector, and luminescence was immediately recorded every second for 10 min in a luminometer (Lumat LB 9507). The maximal luminescence (L_{max}) was determined as described (26). Specifically, cells were lysed with 1% digitonin in the presence of 1 M $CaCl_2$, and a peak of RLU was recorded. Calculation concentration was calculated with Equation 1,

$$[Ca^{2+}] = ((L/L_{max})^{1/3} + [118(L/L_{max})^{1/3}] - 1)/ (7 \times 10^6 - [7 \times 10^6 (L/L_{max})^{1/3}]) \quad \text{(Eq. 1)}$$

where L represents the RLU at a given time point. The base-line calcium concentration of *pmc1* in SC and Me_2SO was ~0.38 μM, and that of *pmr1* was about 0.52 μM.

Methylene Blue Viability Assay—*S. cerevisiae* cells grown in media with and without the specified concentrations of AMD and miconazole were stained with methylene blue (Sigma) taken from a stock of 0.1 mg/ml. 250–300 cells were counted under a light microscope. Dead cells stain blue.

FUN-1 Confocal Microscopy—The Live/Dead yeast viability kit was purchased from Molecular Probes. 50 μl of cells grown overnight in the presence or absence of drugs (as specified in Fig. 5) were incubated in SC medium at 30 °C for 1 h with 4 μM FUN-1 dye, which was diluted in SC from a stock of 200 μM in Me_2SO. Immediately after incubation, the cells were examined under a confocal laser-scanning microscope (PerkinElmer UltraView LCI System) equipped with an inverted × 100 oil immersion objective lens. The fluorescent dye was excited at 488 nm by the krypton/argon laser. Conversion of FUN-1 into cylindrical intravacuolar structures was monitored by recording fluorescent micrographs at emission wavelengths of 600 nm (metabolically active and inactive cells) or 520 nm (metabolically inactive cells only). Pseudocolorization was done with Adobe Photoshop software (Adobe Systems Inc.).

RESULTS

Hypersensitivity of the pmr1 Mutant to Amiodarone—To investigate the role of various calcium transport pathways in mediating drug sensitivity, we compared the growth of individual, isogenic gene deletion mutants in media supplemented with micromolar concentrations of AMD. As shown in Fig. 1*A*,

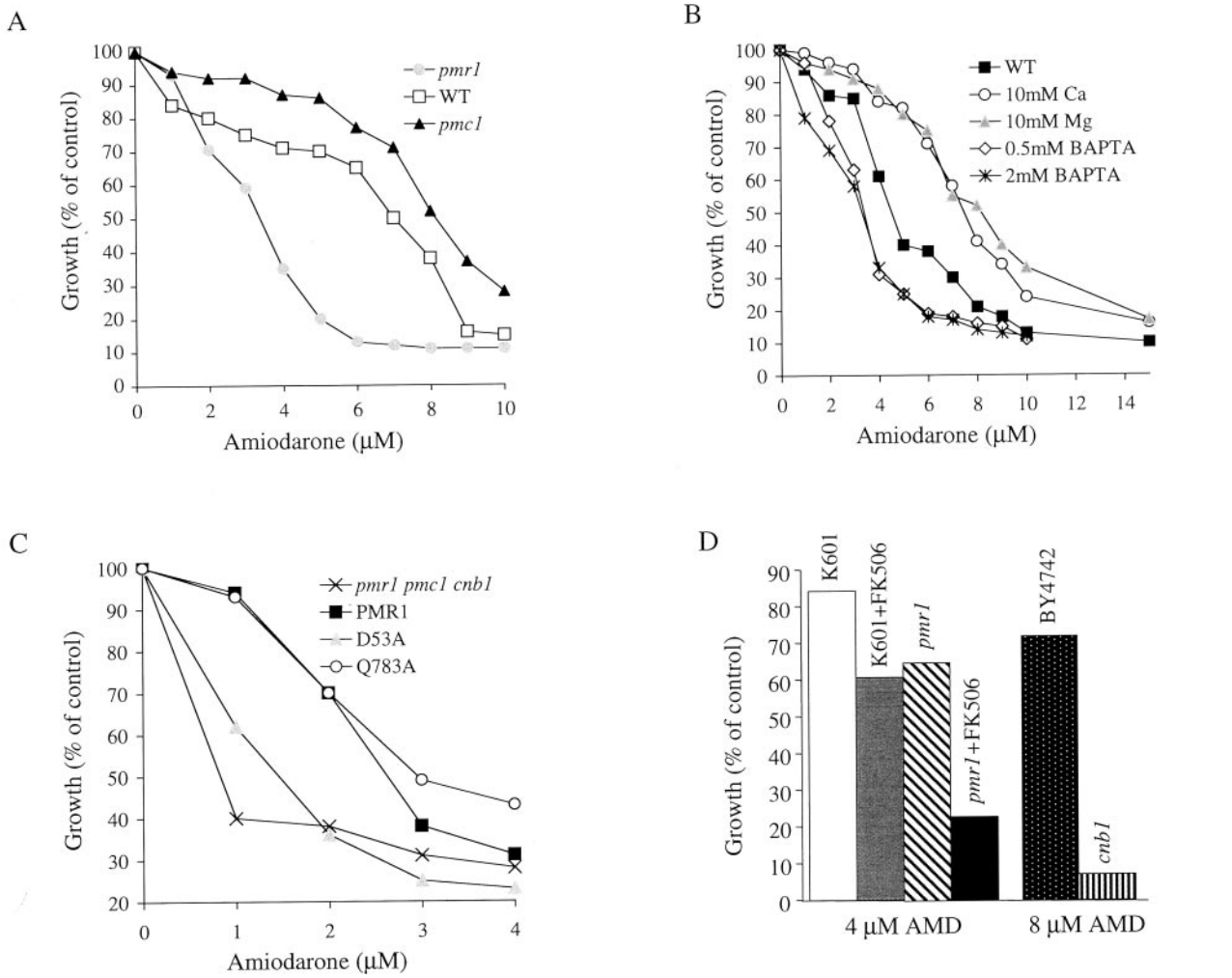

FIG. 1. **AMD sensitivity is modulated by calcium.** *A*, Ca^{2+} pump mutants have differential sensitivities to AMD. Wild-type K601 (WT) and isogenic *pmc1* and *pmr1* mutants were inoculated into 3 ml of SC media supplemented with AMD as shown and grown for 24 h at 30 °C. Growth (optical density at 600 nm) is depicted as percentage of the control culture without drug for each strain. Data points are averages of duplicates, with S.D. values within 5%. One experiment of three is shown. *B*, divalent cations protect against AMD toxicity. Wild-type K601 (WT) cells were grown in AMD-containing SC medium supplemented with one of the following: $CaCl_2$ (10 mM), $MgCl_2$ (10 mM), or BAPTA (0.5 mM or 2 mM) at 30 °C for 24 h. Growth was monitored as described above. *C*, ion selectivity mutants of Pmr1 have differential sensitivities to AMD. Strain K616 (*pmr1pmc1cnb1*) was transformed with a 2μ plasmid carrying wild type Pmr1 or mutants D53A or Q783A and then grown in AMD-supplemented SC medium lacking uracil as described above. Wild type Pmr1 transports both Ca^{2+} and Mn^{2+} equally well, whereas mutant D53A is defective in Ca^{2+} transport, and mutant Q783A is defective in Mn^{2+} transport. *D*, loss of calcineurin increases AMD sensitivity. Pairs of isogenic wild type (K601 or BY4742) and mutant strains (*pmr1* and *cnb1*) were grown in SC media containing 4 or 8 μM AMD, with FK506 (1 μg/ml) added as indicated. Growth was monitored as described above.

the *pmr1* mutant was strikingly more sensitive to AMD; in contrast, the *pmc1* null strain showed a small but reproducible tolerance to the drug, relative to wild type. A survey of deletion mutants of the vacuolar H^+/Ca^{2+} exchanger (*vcx1*) and all known Ca^{2+} channels in yeast (*yvc1*, *cch1*, and *mid1*) revealed a modest exacerbation of AMD sensitivity in both *cch1* and *mid1* mutants but not in the others (not shown). Taken together, these results suggest that some aspect of Ca^{2+} signaling, maintained in large part by the ATP-dependent calcium efflux pump, Pmr1, is important in mediating the growth toxicity of AMD.

Extracellular Calcium Modulates Amiodarone Toxicity—Extracellular calcium has been reported to confer a dose-dependent abrogation of susceptibility to KP4 fungal toxin in the yeast *Ustilago maydis* (28). Here, 10 mM $CaCl_2$ or $MgCl_2$ appeared to protect cell growth against AMD toxicity, whereas BAPTA, a membrane-impermeant cation chelator, enhanced AMD toxicity, consistent with the removal of Ca^{2+} (Fig. 1*B*). Interestingly, the protective effect of increasing Ca^{2+} concentrations (10–25 mM) on AMD sensitivity was most significant in strains lacking Pmr1 (not shown), which may reflect, at least in part, the known dependence of this strain on extracellular Ca^{2+} for optimum growth (29). Mn^{2+} can be a surrogate for Ca^{2+} in a number of physiological processes but was ineffective in conferring protection (data not shown). Monovalent ions (K^+ and Na^+) were previously reported to have little or no effect on AMD toxicity to yeast (1).

Ion Selectivity Mutants of Pmr1 Confirm the Specific Role of Calcium in Amiodarone Toxicity—Since Pmr1 mediates the high affinity transport of both Ca^{2+} and Mn^{2+} into the Golgi (11, 24), it was of interest to determine whether the enhanced sensitivity of *pmr1* mutant to AMD was a consequence of a loss of Ca^{2+} or Mn^{2+} transport. We have previously described two ion selectivity mutants of Pmr1, Q783A and D53A, which show nearly exclusive transport of either Ca^{2+} or Mn^{2+}, respectively (23, 24). These mutants were expressed in a yeast strain devoid of endogenous Ca^{2+} pumps, with the additional deletion of calcineurin to maintain viability (*pmr1pmc1cnb1*) (11, 15). Selective loss of Ca^{2+} transport in Pmr1 mutant D53A resulted in loss of tolerance to AMD, similar to the host strain lacking

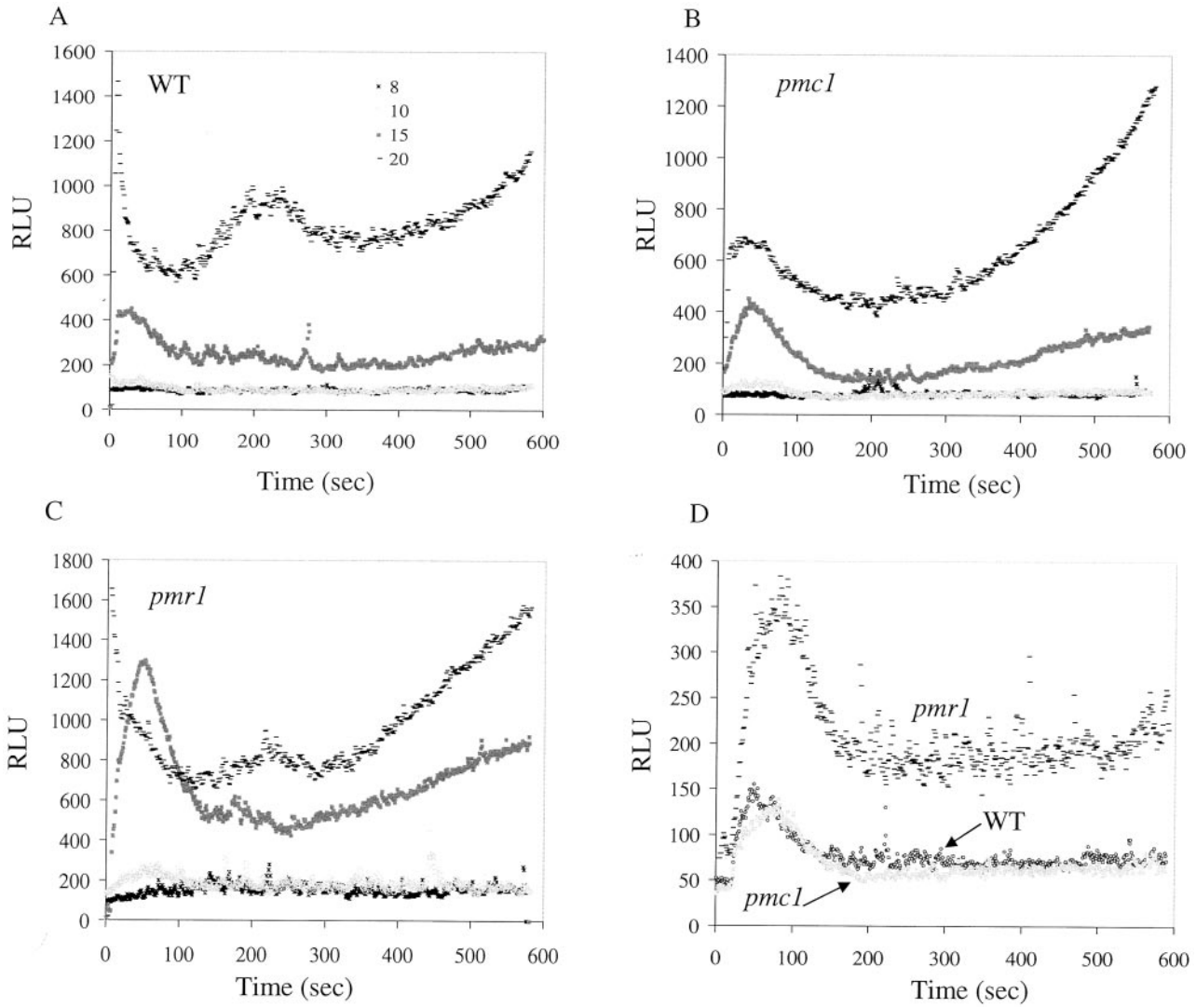

FIG. 2. **AMD-induced cytoplasmic Ca^{2+} elevation is biphasic and elevated in the *pmr1* mutant.** Ca^{2+}-dependent luminescence of the aequorin-coelenterazine photoprotein complex expressed in the cytosol of WT (*A*), *pmc1* (*B*), and *pmr1* (*C*) mutants was measured upon the addition of AMD (8–20 μM) to cells resuspended in SC medium at 1 OD/ml, as described under "Experimental Procedures." *Symbols* corresponding to the AMD concentrations are shown in the *inset* to *A*. Luminescence (RLU) is measured in arbitrary units/s, over 10 min. Calibration of RLU to free calcium concentration is described under "Experimental Procedures." *D*, a comparison of luminescence in response to 10 μM AMD. The *pmr1* mutant shows greater elevations of aequorin luminescence, relative to WT and *pmc1*.

Pmr1 and Pmc1 (Fig. 1*C*). In contrast, selective loss of Mn^{2+} transport of mutant Q783A did not alter AMD sensitivity. These results are consistent with the inability of extracellular Mn^{2+} to protect against AMD toxicity, and they establish the specific role of Ca^{2+} ions in mediating the cellular effects of the drug.

Loss of Calcineurin Function Enhances Toxicity of Amiodarone—Calcineurin has been shown to be nonessential for normal growth but critical for survival during membrane stress in *C. albicans* (*3*). The enhanced AMD sensitivity of the triple mutant, *pmr1pmc1cnb1* (Fig. 1*C*) relative to the individual gene deletions (Fig. 1*A*) suggested that loss of calcineurin may be synergistic with loss of the Golgi Ca^{2+} pump Pmr1. To confirm this, we investigated the effect of FK506 (1 μg/ml), a potent inhibitor of calcineurin, on the AMD sensitivity of wild type and *pmr1* strains (Fig. 1*D*). As predicted, the addition of FK506 exacerbated the AMD sensitivity of the *pmr1* mutant. Additionally, the *cnb1* mutant, lacking functional calcineurin, displayed increased sensitivity to AMD at higher concentrations of the drug (Fig. 1*D*). Taken together, these data confirm the importance of calcineurin in the Ca^{2+} signaling pathway involved in drug sensitivity.

Amiodarone Triggers Calcium Influx in Yeast Cells—Next, we investigated whether AMD induced calcium entry into yeast and whether calcium entry correlated with drug sensitivity. Calcium-dependent luminescence of the aequorin-coelenterazine photoprotein complex was monitored in the first few minutes immediately following drug addition. In all strains examined, application of AMD resulted in a biphasic elevation of cytoplasmic calcium that was dependent on AMD concentration (Fig. 2, *A–C*). The first peak of calcium occurred extremely fast (within 1–1.5 min) and was followed by a sustained rise that lasted for the duration of the assay. The magnitude of both phases, as well as the kinetics of the initial elevation was steeply dependent on AMD concentration, with maximal increase observed between 10 and 20 μM AMD. Elevation of cytosolic calcium was found to correlate with AMD sensitivity; thus, the addition of 10 μM AMD elicited the largest luminescence changes in the *pmr1* mutant, whereas the *pmc1* mutant showed similar changes relative to wild type (Fig. 2*D*). Estimated cytosolic calcium concentrations of the initial peak, based on the calibration described under "Experimental Procedures," reached 0.7 μM in wild type and *pmc1* and close to 1 μM in *pmr1* cells; the second sustained rise remained around 0.5

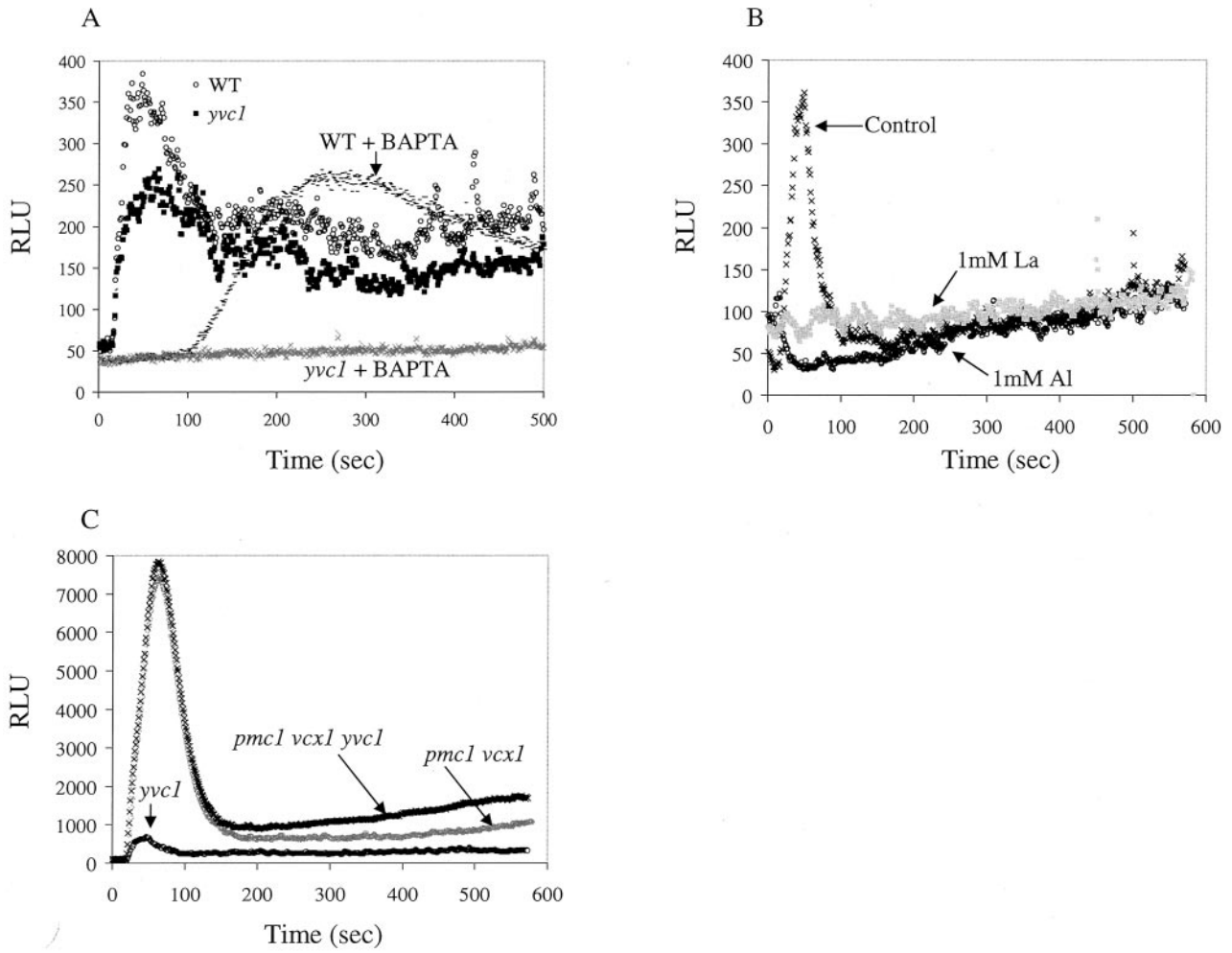

FIG. 3. **Contribution of extracellular and vacuolar stores to AMD-induced Ca^{2+} elevations.** *A*, aequorin luminescence of K601 (WT) and the isogenic *yvc1* mutant was monitored upon the addition of 15 μM AMD to cells resuspended at a concentration of 1 OD/ml in SC medium with or without BAPTA (5 mM), as indicated. *B*, the addition of 1 mM Al^{3+} or La^{3+} to wild type cells immediately prior to measurement of aequorin luminescence blocked the initial influx of Ca^{2+} but not the slower rise. All traces were in response to 15 μM AMD; the control trace had no ions added. *C*, the initial peak of luminescence measured in response to 15 μM AMD in *pmc1vcx1* and *pmc1vcx1yvc1* mutants showed a large (14-fold) increase in magnitude relative to an isogenic control strain (*yvc1*).

μM for WT and *pmc1* but stayed at 0.75 μM for *pmr1*.

Ca^{2+} Entry in Response to AMD Comes from Extracellular and Intracellular Stores—It was of interest to determine the relative contribution of extracellular and intracellular Ca^{2+} stores to the biphasic elevations of cytosolic Ca^{2+} observed in Fig. 2. When we used the membrane-impermeant cation chelator BAPTA (5 mM) to deplete extracellular Ca^{2+}, the first peak of AMD-induced aequorin luminescence in wild type cells was eliminated, indicating that external calcium contributed to the rapid, initial rise in cytoplasmic calcium (Fig. 3*A*). Following a short lag, a broad, sustained rise was observed in BAPTA-treated cells that probably corresponded to the second phase of luminescence seen in the absence of BAPTA. These results implied that Ca^{2+} release from intracellular stores must contribute to cytosolic elevation of Ca^{2+} and, further, that Ca^{2+} entry from extracellular sources is not required to trigger release from stores. The transient receptor potential-like channel Yvc1 has been shown to mediate Ca^{2+} release from the vacuole in response to hypertonic shock (30). We investigated the contribution of vacuolar Ca^{2+} release by examining aequorin luminescence in the *yvc1* mutant (Fig. 3*A*). The changes in intracellular Ca^{2+} in the *yvc1* mutant were essentially similar to wild type in the absence of BAPTA. The first peak of wild type cells reached ~0.8–0.9 μM, and that of *yvc1* was about 0.7 μM. The second sustained rise in both strains ranged from 0.59 to 0.66 μM of free calcium. Strikingly, BAPTA treatment completely abolished Ca^{2+} elevation in the *yvc1* mutant. These results indicate that whereas the first peak of AMD-induced cytosolic Ca^{2+} comes exclusively from outside, the later elevation derives from both extracellular and vacuolar sources.

Courchesne and Ozturk reported that Mid1 could be the channel through which AMD-induced calcium entry occurs. They showed that the Ca^{2+} transient in *mid1* mutant was 5-fold lower than the wild type control although not abolished (2). In Fig. 3*B*, we show that the addition of the calcium channel blockers La^{3+} or Al^{3+} abolished the first elevation of Ca^{2+} but not the second, reaffirming the conclusion from Fig. 3*A* that the initial rise in luminescence comes solely from extracellular Ca^{2+}, whereas the slower increase is derived from both extracellular and intracellular stores. High concentrations (10 mM) of extracellular Ca^{2+} or Mg^{2+} also diminished the initial peak, possibly due to desensitization/inactivation of the putative plasma membrane channel (not shown).

Figs. 2 and 3 present the initial elevation of cytosolic Ca^{2+} being rapidly reversed within the first 1–1.5 min after AMD exposure. In *pmr1*, the initial rise of calcium is higher, and the decay is slower (Fig. 2*D*), suggesting that active Ca^{2+} transport into the Golgi/secretory pathway by the Pmr1 pump contributes in part to the decay of aequorin luminescence. Since the vacuole is known to be the major store for cellular calcium, we

TABLE I
Genome-wide screen of single gene deletions for AMD-sensitive strains

Almost 5000 mutants, each of which lacks a nonessential gene, were grown in YPD supplemented with 7 μM AMD as described under "Experimental Procedures." 36 mutants were identified with enhanced sensitivity to AMD and classified to distinct functional classes according to the *Saccharomyces* Genome Database (SGD, Stanford University).

Mutant types	Mutants
Transporters	*pmr1, pdr5, cup5/vma3, vma13, vma1*
Ergosterol biosynthesis	*erg3, erg6, erg24*
Trafficking pathways	*rcy1, vps65, vps16, vps45, cog6*
Kinases/phosphatases	*slt2, ypk1, sac1, opi1, ptc1*
Pleiotropic drug-sensitive mutants	*lem3, cdc50*
Transcription factors	*swi3, rtf1, rrn10, uga3*
Others	*pai3, elg1, nbp2*
Unknowns	*YMR299C, ps110, YHR155W, YHR035W, rai1, YBL083C, YMR122C, YDR271C, YOL087C*

hypothesized a significant contribution of vacuolar Ca^{2+} sequestration in response to AMD-induced calcium influx. Indeed, we saw that in the absence of both known vacuolar Ca^{2+} transporters, Vcx1 and Pmc1, the first luminescent peak corresponding to extracellular Ca^{2+} uptake was greatly elevated (Fig. 3*C*), with an estimated maximum of 3.3 μM (concentration calculation described under "Experimental Procedures"). This is consistent with a prominent role for vacuolar sequestration in the Ca^{2+} homeostatic mechanism. The disruption of all three known Ca^{2+} removal pathways, Pmr1, Pmc1, and Vcx1, is known to be nonviable (14), most likely due to a complete loss of cytosolic Ca^{2+} homeostasis.

Large Scale Screen of a Yeast Deletion Library for Amiodarone-sensitive Mutants—The *S. cerevisiae* gene deletion library offers a powerful tool for the assignment of new functions to sequenced genes. Since AMD is a novel antimycotic with unknown targets in yeast, it was of interest to identify additional genes contributing to AMD sensitivity that might lead to further insight into the cellular mechanism of AMD-mediated toxicity. We twice screened a library of nearly 5000 single, nonessential gene deletions for hypersensitivity to AMD (see "Experimental Procedures"). 15 mutants were identified in the first screen, and 21 more were found in the second screen. They were all retested several times to confirm their drug-sensitive phenotype (Table I). The identification of *pmr1* from this genome-wide screen provided independent verification of the results shown in Fig. 1*A*. We also found *pdr5*, a mutant lacking the pleiotropic drug resistance ATPase and widely known to be hypersensitive to a variety of cytotoxic agents (31). Pdr5 is likely to be involved in detoxification of AMD by mediating drug efflux from the cell. Deletion of individual subunits of the vacuolar H^+-ATPase (*vma1*, *vma3*, and *vma13*) abolishes the vacuolar proton electrochemical gradient, which in turn, is likely to limit vacuolar calcium sequestration. The other isolates fell into clusters that include mutants deficient in components of the ergosterol biosynthesis pathway, intracellular trafficking pathways, lipid signaling and kinases, transcription factors, and genes with unknown functions. Some of these strains have been shown previously to have pleiotropic sensitivity to drugs and may be involved with AMD toxicity in a more general rather than specific way. For example, *lem3* and *cdc50* mutants have deletions in homologous genes of unknown function and are known to be more sensitive to brefeldin A (32) and methyl methanesulfonate and hydroxylurea (33), respectively. The ergosterol biosynthesis pathway is the primary target of many antifungals (34), and disruption of this pathway damages the integrity of the cell membrane. It was therefore not surprising to find *erg* mutants (*erg3*, *erg6*, and *erg24*) with enhanced sensitivity to AMD. However, the discovery of mutants defective in various components of intracellular trafficking pathways, such as *cog6*, *vps16*, *vps45*, *vps65*, and *rcy1* was unexpected. We speculate that mutations in trafficking and signaling pathways might indirectly disrupt Ca^{2+} homeostasis, resulting in hypersensitivity to AMD.

Based on our results thus far, we have suggested a correlation between AMD sensitivity and increased Ca^{2+} levels in the cytoplasm. We sought to confirm this hypothesis by examining calcium-dependent luminescence of aequorin in three representative mutants identified from the genome-wide screen for AMD hypersensitivity. As shown in Fig. 4, all three mutants chosen (*vma3*, *vps45*, and *rcy1*) displayed substantially higher elevations of cytosolic Ca^{2+} upon the addition of AMD despite the differences in their individual cellular roles. *vma3* lacks the H^+-transporting subunit *c* of the vacuolar H^+-ATPase (35); *vps45* is a vacuolar protein sorting mutant defective in Golgi- or cytosol-to-vacuole transport (36), and *rcy1* is important for endocytosis/recycling at the plasma membrane (37). In the *vma3* and *vps45* mutants, upon the addition of AMD the first peak of aequorin luminescence is elevated up to 1.2 μM and broadened, suggesting that defects in the function and biogenesis of the vacuole compromise its ability to effectively sequester Ca^{2+} (Fig. 4*A*). The *rcy1* mutant had a unique response to AMD, showing significant increases in both luminescence phases such that the first peak, which reached an estimated Ca^{2+} concentration of 2 μM, was not completely abolished before the greatly amplified, second phase occurred (Fig. 4*B*). To determine whether the second elevation of calcium in this mutant came from external sources, we examined aequorin luminescence in the presence of BAPTA, added to chelate extracellular calcium. As seen in other strains (Fig. 3), we showed that the first peak of cytosolic Ca^{2+} was abolished upon BAPTA treatment, but the second, sustained elevation of Ca^{2+} remained (Fig. 4*B*). Our results suggest AMD-induced release of Ca^{2+} from internal stores, possibly the vacuole, cannot be effectively cleared from the cytoplasm in the *rcy1* mutant. Alternatively, Ca^{2+}-filled vesicles derived from the Golgi may require the function of the Rcy1 protein for exocytic unloading.

Synergism between AMD and Azoles—Conventional azole antifungals, such as miconazole (MIC) and fluconazole (FLUC), arrest cell growth and are therefore fungistatic rather than fungicidal. A major problem in the long term treatment with azoles is the appearance of resistant fungi. AMD has been reported to have broad range fungicidal effects, particularly against *Cryptococcus* (1), although the reported minimal inhibitory concentrations may be too high to be practical for treatment without adverse side effects. We first tested the effect of low concentrations of AMD (2–4 μM) on cell viability of *Saccharomyces* in the presence of therapeutic doses of miconazole (1 μM). After 24 h of exposure, neither drug alone had significant effect on cell viability, as determined by methylene blue staining (Fig. 5*A*). The synergistic effect of the two drugs was seen at all concentrations tested and is shown at 4 μM AMD; cell survival fell dramatically from close to 100% in AMD or MIC alone to less than 10% in the presence of both drugs. To examine the metabolic state of drug-treated yeast, cells were stained with the fluorescent dye FUN-1. Without drugs, the cells were metabolically active and able to process FUN-1 into cylindrical intravacuolar structures (Fig. 5*B*). On the other hand, when grown in the combined presence of AMD (4 μM) and MIC (1 μM) for 24 h, nearly all cells turned metabolically quiescent, and FUN-1 remained a green-yellow, diffused stain in the cytoplasm (Fig. 5*C*).

Similar findings were observed using the pathogenic yeasts *C. albicans* and *C. neoformans* (Fig. 6). As reported (1), AMD

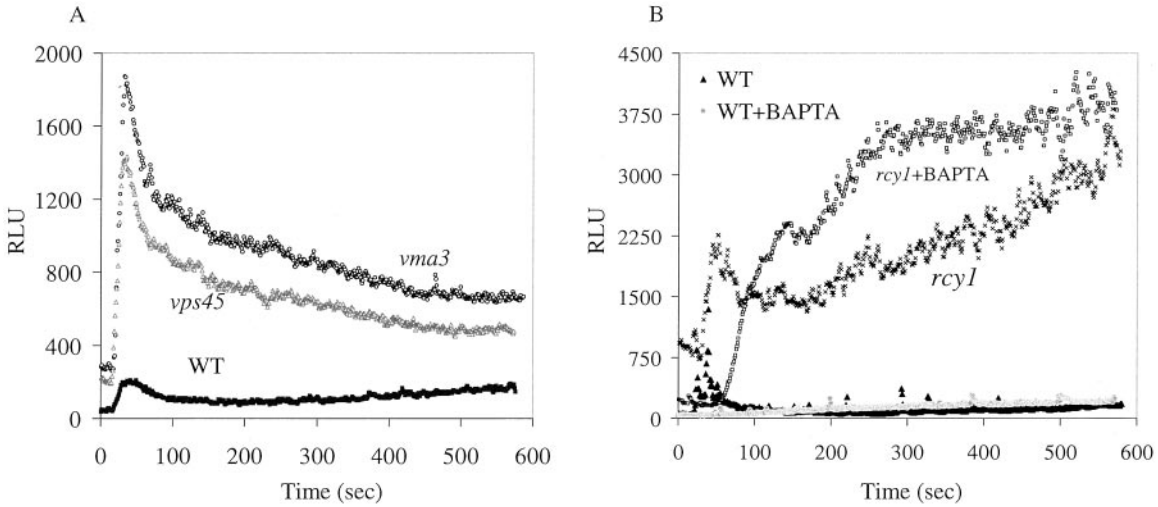

FIG. 4. **AMD-sensitive *vma3*, *vps45*, and *rcy1* strains cannot effectively clear Ca^{2+} from the cytosol.** Isogenic wild type BY4742 (WT) and mutant strains were treated with 15 μM AMD immediately prior to measurement of aequorin luminescence as described under "Experimental Procedures." *A*, the initial peak of Ca^{2+} is greatly elevated (and its subsequent decay is slowed) in *vma3* and *vps45* mutants, relative to WT. *B*, in the *rcy1* mutant, both phases of cytosolic Ca^{2+} entry are greatly elevated, relative to WT. The addition of BAPTA (5 mM) to the cultures immediately prior to AMD supplement abolished the first peak of Ca^{2+} in both WT and *rcy1* but not the second, slower elevation.

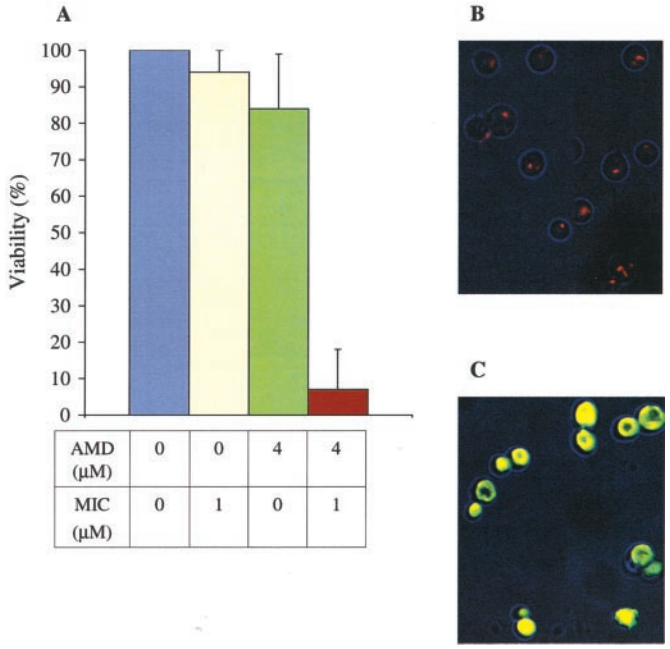

FIG. 5. **Synergism between amiodarone and miconazole in *S. cerevisiae*.** *A*, wild type *S. cerevisiae* (BY4742) was grown in SC medium in the absence or presence of AMD (4 μM), or MIC (1 μM), individually or in combination. After 24 h, the cells were stained with methylene blue and counted as described under "Experimental Procedures." Viability was calculated as the number of unstained cells divided by the total number of cells counted (about 250–300), expressed as a percentage. The average of three separate experiments is shown. *B* and *C*, wild type cells (BY4742) were grown overnight in SC medium without (*B*) and with both drugs (*C*) and then stained with 4 μM FUN-1 for 1 h at 30 °C. Final concentrations of AMD and MIC were 4 μM and 1 μM, respectively. Excitation wavelength was 488 nm, and emission was at 520 and 600 nm.

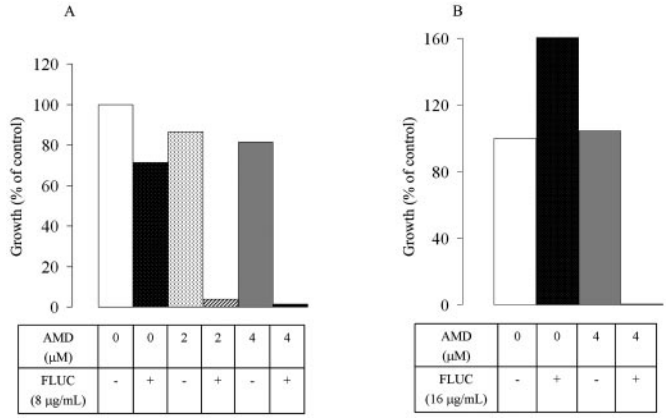

FIG. 6. **Synergism between amiodarone and fluconazole in pathogenic fungi.** *A*, *C. albicans* SC5314 was grown in 1 ml of YPD supplemented with 2 μM and 4 μM AMD in the presence or absence of 8 μg/ml FLUC at 37 °C. After 20 h, 5 μl of cells were diluted into 1.5 ml of drug-free YPD and grown at 37 °C for another 20 h. Growth (absorbance at 600 nm) was plotted as a percentage of control (no drug). Data points are averages of duplicates, with S.D. less than 5%. *B*, *C. neoformans* JEC21 was grown in 5 ml of YPD at 30 °C, shaken vigorously for 20 h. The medium had 4 μM AMD with or without 16 μg/ml FLUC. 5 μl of cells exposed to AMD alone or 20 μl of cells exposed to both drugs were diluted into 10 ml of YPD and grown for 24–48 h at 30 °C until saturation. Growth was measured as optical density at 600 nm and then plotted as a percentage of control (no drug). Data points are averages of duplicates, with S.D. equal to or less than 10%.

inhibited growth of both yeasts, whereas an effective dose of FLUC (8 or 16 μg/ml) completely prevented cell growth (not shown). Following a 20-h exposure to drugs, cells previously exposed to low levels of AMD (2 or 4 μM) or to FLUC (8 or 16 μg/ml) alone essentially recovered in drug-free medium, growing to levels approaching control (uninhibited) levels. In contrast, the combination of drugs inhibited regrowth of *C. albicans* (Fig. 6*A*) and *C. neoformans* (Fig. 6*B*) by 95–98%, indicative of an effective loss of viability. It should be noted that therapeutic plasma levels of 4 μM have been reported for AMD and its metabolite, desethylamiodarone (1), suggesting that these clinically relevant doses may be additionally effective in antifungal therapy.

DISCUSSION

AMD is an important therapeutic agent used in the treatment of life-threatening ventricular arrhythmias and supraventricular dysrhythmias (38). AMD and its active metabolite, desethylamiodarone, are unusual in their long biological half-life (25–110 days) and their broad range of targets. In cardiac cells, AMD inhibits ion channels such as L-type Ca^{2+} channels and Na^+ and K^+ channels, thus prolonging the duration of action potential (39). Although the therapeutic benefits of AMD are well established, toxic side effects occur in

noncardiac tissues, most prominently the lungs and the thyroid gland. There is evidence that AMD causes apoptosis in thyrocytes (40) and pneumocytes (41). Alveolar macrophages treated with AMD show defects in endocytosis at the steps after the late endosome and missort lysosomal enzymes to the plasma membrane (42). Of particular interest to this study are the reports of acute AMD exposure leading to a sustained cytoplasmic Ca^{2+} rise in synaptosomes (43) and in aortic or pulmonary endothelial cells (44, 45). Our work demonstrates a correlation between AMD toxicity and increased cytoplasmic Ca^{2+} levels in *S. cerevisiae*, exemplifying the conservation of Ca^{2+} transport and signaling pathways between yeast and higher eukaryotes. Therefore, a better understanding of the cellular basis of AMD toxicity in this simple model organism is relevant to understanding and eventually circumventing the toxic side effects of the drug in humans.

We show that low, micromolar doses of AMD, in the range where growth inhibition is observed, stimulate Ca^{2+} uptake through a plasma membrane channel that is inhibited by Ca^{2+} channel blockers such as Al^{3+} and La^{3+} and by competition with Mg^{2+} ions. Courchesne and Ozturk (2) have suggested that one pathway for Ca^{2+} entry is the stretch-activated channel Mid1. They found that the *mid1* mutant was less sensitive to AMD than *cch1*, suggesting that loss of Cch1 allows Mid1 to function independently. However, we find that the *mid1* mutant exhibits enhanced growth sensitivity to AMD similar to that of the *cch1* mutant (not shown). The reason for this discrepancy is not clear and warrants further studies.

We provide new evidence for Ca^{2+} release from the vacuole via the transient receptor potential-like channel, Yvc1. Taken together with a previously published report of the role of this channel in mediating the response to hypertonic shock (30), it would appear that Yvc1 is the major release mechanism for intracellular stores of Ca^{2+} in yeast. Whereas depletion of extracellular Ca^{2+} or the addition of Ca^{2+} channel blockers abolished the immediate elevation of cytosolic Ca^{2+}, they did not prevent the Yvc1-mediated release from vacuolar stores, which continued to increase during the time course of the assay. Based on our calculations of calcium concentration, the two phases in WT cells were estimated to correspond to 0.7 and 0.5 μM free Ca^{2+}, respectively, in response to 10 μM AMD. In strains hypersensitive to AMD, such as *rcy1*, these values increased to 2 μM and 1.6–2.5 μM, respectively. We speculate that it is the second sustained rise of cytoplasmic Ca^{2+} that eventually becomes toxic to AMD-treated cells. Given that the sequence of calcium entry from extracellular sources clearly precedes that from intracellular stores in our experiments, we can rule out a role for capacitative calcium entry in the immediate response to AMD, although such mechanisms are likely to contribute to the sustained phase of calcium increase.

It is well known that excessive cytosolic Ca^{2+} is toxic (46), and indeed, we show a consistent correlation between hypersensitivity to AMD and excessive elevation of cytosolic Ca^{2+}. For example, in the absence of the Golgi Ca^{2+} pump, Pmr1, elevated Ca^{2+} levels in response to AMD result in a hypersensitive phenotype, consistent with the important role of this pump in the dynamic regulation of cellular Ca^{2+} levels. Among the deletion strains that we analyzed, only the pmc1 mutant was moderately tolerant to AMD and was seen to have similar elevations of cytosolic Ca^{2+}, relative to wild type. Paradoxically, very high levels (10 mM) of extracellular Ca^{2+} or Mg^{2+} ameliorated the adverse effects of AMD (1) (Fig. 2*A*), seemingly in contradiction to our hypothesis. A possible explanation is that the Ca^{2+} influx pathway(s), probably a Ca^{2+} channel, is down-regulated in the presence of excess amounts of extracellular Ca^{2+}. A similar response has been observed in *Nicotiana* cells exposed to *Phytophthora* toxins (10), in which calcium influx first increased and then decreased with increasing extracellular Ca^{2+} levels.

In order to gain insight into the molecular target(s) of AMD in yeast, we have defined distinct cellular pathways and components that confer drug sensitivity upon disruption (Table I). The genome-wide screens were not exhaustive, and it is possible that many other mutants were missed. However, our results are promising, since we have identified several interesting mutants (*e.g. erg3*, *rcy1*, *vps45*) that, with further studies, would shed more light on the molecular basis of AMD toxicity as well as calcium homeostasis in fungi. The enhanced sensitivity of trafficking mutants may be due to defects in drug detoxification and/or Ca^{2+} clearance via the secretory pathway or vacuolar sequestration. For example, the *rcy1* mutant is defective in exit from an early, sorting endosome which has been postulated to receive traffic from the secretory and endocytic pathways (37). AMD toxicity in the *rcy1* mutant might be due to defective traffic of Golgi- or vacuole-derived vesicles loaded with Ca^{2+} or in the recycling of endocytosed AMD to the plasma membrane. On the other hand, *vps45*, a Golgi- or cytosol-to-vacuole transport mutant (36), and *vma3*, a strain lacking the proton-transporting subunit c of the vacuolar H^+-ATPase (35), are both defective in vacuolar function and biogenesis, so that Ca^{2+} cannot be effectively sequestered. The drug sensitivity observed in signaling mutants like *sac1* and *ptc1* is also interesting and unexpected. SAC1 encodes a phosphoinositide phosphatase, in the absence of which the cell contains an irregularly shaped vacuole surrounded by lipid droplets (47), suggesting that vacuolar function is compromised in this mutant. Ptc1 is a negative regulator of the high osmolarity glycerol pathway and has been shown to maintain the basal kinase activity of Hog1 (48). Clearly, our findings warrant further investigation to elucidate the relationships between AMD toxicity and *PTC1* as well as other genes identified in the screen.

It remains to be determined if AMD directly binds and affects a Ca^{2+} channel or disrupts an intracellular signaling pathway that then leads to cytosolic Ca^{2+} entry. We note that in addition to its action on ion channels, other reported cellular activities of AMD and desethylamiodarone encompass binding and activation of heterotrimeric G proteins (49), inhibition of phospholipases A1 and A2 (50), and binding and inhibition of calmodulin (51, 52) as well as protein kinase C (53). In any case, our work suggests the possibility of using AMD as a novel, broad range antimycotic that is likely to be effective against even drug-resistant pathogenic fungi. Most, if not all, of the cellular pathways and components identified in our screen for mutants hypersensitive to this drug (Table I) are expected to be conserved in the pathogenic counterparts of bakers' yeast. Mucosal and systemic fungal infections are among the main killers in immunocompromised patients, and resistant fungi have become increasingly prevalent. Conventional drugs such as the azoles are only fungistatic, whereas others that are fungicidal, such as the polyenes, have harmful side effects that preclude long term treatment (54). The target of both azoles and polyenes is ergosterol and its biosynthesis pathway. One mechanism of drug resistance is the inactivation of Erg3, a sterol desaturase, which results in the accumulation of 14α-methylfecosterol, a growth-promoting sterol (55). In the absence of ergosterol, the *erg3* mutant is resistant to both amphotericin B (a polyene) and azoles. Interestingly, the *erg3* mutant was identified in our screen for AMD sensitivity (Table I), suggesting that cytotoxicity of AMD occurs by a mechanism distinct from that of the conventional antifungals. If added to an antifungal regimen, AMD could potentially enhance the efficacy by

eliminating cells whose growth is only halted by the other fungistatic drugs. In combination, specificity against pathogenic fungi would be conferred by the azoles, and toxicity would be conferred by AMD. To be useful therapeutically, the low concentrations of AMD that are synergistic with azoles should have minimal toxicity to humans.

Although the strategy of combining different classes of antifungals is theoretically attractive, some drugs, when used concomitantly or sequentially, exert no synergism and may even be antagonistic. Specifically, *A. fumigatus*, when pretreated with noninhibitory doses of itraconazole (an azole), developed resistance to amphotericin B (a polyene) (56). A combination of fluconazole (an azole) and caspofungin or anidulafungin (two echinocandins) produced no significant changes in efficacy of individual drugs, although the former targets the ergosterol biosynthesis pathway, whereas the latter two inhibit cell wall synthesis (54). Therefore, the strong synergism between miconazole or fluconazole and AMD demonstrated in this work promises a potentially effective regimen against severe and life-threatening fungal infections.

Acknowledgments—S. S.G. thanks Dr. C. M. C. Allen and Dr. R. Jones of Lucy Cavendish College for making the elective research possible. We thank Dr. B. Cormack (The Johns Hopkins University School of Medicine) for the kind gifts of fluconazole and *C. albicans* and Dr. J. Heitman (Duke University Medical Center) for *C. neoformans*.

REFERENCES

1. Courchesne, W. E. (2002) *J. Pharmacol. Exp. Ther.* **300,** 195–199
2. Courchesne, W. E., and Ozturk, S. (2003) *Mol. Microbiol.* **47,** 223–234
3. Cruz, M. C., Goldstein, A. L., Blankenship, J. R., Del Poeta, M., Davis, D., Cardenas, M. E., Perfect, J. R., McCusker, J. H., and Heitman, J. (2002) *EMBO J.* **21,** 546–559
4. Matsumoto, T. K., Ellsmore, A. J., Cessna, S. G., Low, P. S., Pardo, J. M., Bressan, R. A., and Hasegawa, P. M. (2002) *J. Biol. Chem.* **277,** 33075–33080
5. Bonilla, M. Nastase, K. K., and Cunningham, K. W. (2002) *EMBO J.* **21,** 2343–2353
6. Edlind, T., Smith, L., Henry, K., Katiyar, S., and Nickels, J. (2002) *Mol. Microbiol.* **46,** 257–268
7. Locke, E. G., Bonilla, M., Liang, L., Takita, Y., and Cunningham, K. W. (2000) *Mol. Cell. Biol.* **20,** 6686–6694
8. Andjelic, S., Khanna, A., Suthanthiran, M., and Nikolic-Zugic, J. (1997) *J. Immunol.* **158,** 2527–2534
9. Kurzweilova, H., and Sigler, K. (1993) *Folia Microbiol.* **38,** 524–526
10. Lecourieux, D., Mazars, C., Pauly, N., Ranjeva, R., and Pugin, A. (2002) *Plant Cell* **14,** 2627–2641
11. Sorin, A., Rosas, G., and Rao, R. (1997) *J. Biol. Cell* **272,** 9895–9901
12. Marchi, V., Sorin, A. Wei, Y., and Rao, R. (1999) *FEBS Lett.* **454,** 181–186
13. Ton, V.-K., Mandal, D., Vahadji, C., and Rao, R. (2002) *J. Biol. Chem.* **277,** 6422–6427
14. Cunningham, K. W., and Fink, G. R. (1996) *Mol. Cell. Biol.* **16,** 2226–2237
15. Cunningham, K. W., and Fink, G. R. (1994) *J. Cell Biol.* **124,** 351–363
16. Pozos, T. C., Sekler, I., and Cyert, M. S. (1996) *Mol. Cell. Biol.* **16,** 3730–3741
17. Miseta, A., Kellermayer, R., Aiello, D. P., Fu, L., and Bedwell, D. M. (1999) *FEBS Lett.* **451,** 132–136
18. Palmer, C. P., Zhou, X. L., Lin, J., Loukin, S. H., Kung, C., and Saimi, Y. (2001) *Proc. Natl. Acad. Sci. U. S. A.* **98,** 7801–7805
19. Paidhungat, M., and Garrett, S. (1997) *Mol. Cell. Biol.* **17,** 6339–6347
20. Muller, E. M., Locke, E. G., and Cunningham, K. W. (2001) *Genetics* **159,** 1527–1538
21. Cyert, M. S. (2001) *Annu. Rev. Genet.* **35,** 647–672
22. Fox, D. S., and Heitman, J. (2002) *Bioessays* **24,** 894–903
23. Mandal, D., Woolf, T., and Rao, R. (2000) *J. Biol. Cell* **273,** 23933–23938
24. Wei, Y., Chen, J., Rosas, G., Tompkins, D. A., Holt, A., and Rao, R. (2000) *J. Biol. Chem.* **275,** 23927–23932
25. Fonzi, W. A., and Irwin, M. Y. (1993) *Genetics* **134,** 717–728
26. Cruz, M. C., Goldstein, A. L., Blankenship, J., Poeta, M. D., Perfect, J. R., McCusker, J. M., Bennani, Y. L., Cardenas, M. E., and Heitman, J. (2001) *Antimicrob. Agents. Chemother.* **45,** 3162–3170
27. Allen, D. G., Blinks, J. R., and Prendergast, F. G. (1977) *Science* **195,** 996–998
28. Gage, M. J., Bruenn, J., Fischer, M., Sanders, D., and Smith, T. J. (2001) *Mol. Microbiol.* **41,** 775–785
29. Durr, G., Strayle, J., Plemper, R., Elbs, S., Klee, S. K., Catty, P., Wolf, D. H., and Rudolph, H. K. (1998) *Mol. Biol. Cell* **9,** 1149–1162
30. Denis, V., and Cyert, M. S. (2002) *J. Cell Biol.* **156,** 29–34
31. Bauer, B. E., Wolfger, H., and Kuchler, K. (1999) *Biochim. Biophys. Acta.* **1461,** 217–236
32. Sitcheran, R., Emter, R., Kralli, A., and Yamamoto, K. R. (2000) *Genetics* **156,** 963–972
33. Moir, D., Stewart, S. E., Osmond, B. C., and Botstein, D. (2000) *Genetics* **100,** 547–563
34. Tkacz, S., and DiDomenico, B. (2001) *Curr. Opin. Microbiol.* **4,** 540–545
35. Eide, D. J., Bridgham, J. T., Zhao, Z., and Mattoon, J. R. (1993) *Mol. Gen. Genet.* **241,** 447–456
36. Abeliovich, H., Darsow, T., and Emr, S. D. (1999) *EMBO J.* **18,** 6005–6016
37. Wiederkehr, A., Avaro, S., Prescianotto-Baschong, C., Haguenauer-Tsapis, R., and Riezman, H. (2000) *J. Cell Biol.* **149,** 397–410
38. Stevenson, W. G., Ellison, K. E., Sweeney, M. O., Epstein, L. M., and Maisel, W. H. (2002) *Cardiol. Rev.* **10,** 8–14
39. Kodama, I., Kamiya, K., and Toyama, J. (1999) *Am. J. Cardiol.* **84,** 20R–28R
40. Di Matola, T., D'Ascoli, F., Fenzi, G., Rossi, G., Martino, E., Bogazzi, F., and Vitale, M. (2000) *J. Clin. Endocrinol. Metab.* **85,** 4323–4330
41. Bargout, R., Jankov, A., Dincer, E., Wang, R., Komodromos, T., Ibarra-Sunga, O., Filippatos, G., and Uhal, B. D. (2000) *Am. J. Physiol.* **278,** L1039–L1044
42. Baritussio, A., Marzini, S., Agostini, M., Alberti, A., Cimenti, C., Bruttomesso, D., Manzato, E., Quaglino, D., and Pettenazzo, A. (2001) *Am. J. Physiol.* **281,** L1189–L1199
43. Kodavanti, P. R., Pentyala, S. N., Yallapragada, P. R., and Desaiah, D. (1992) *Naunyn Schmiedeberg's Arch. Pharmacol.* **345,** 213–221
44. Himmel, H. M., Dobrev, D., Grossmann, M., and Ravens, U. (2000) *Naunyn Schmiedeberg's Arch. Pharmacol.* **362,** 489–496
45. Powis, G., Olsen, R., Standing, J. E., Kachel, D., and Martin, W. J., II (1990) *Toxicol. Appl. Pharmacol.* **103,** 156–164
46. McConkey, D. J., and Orrenius, S. (1997) *Biochem. Biophys. Res. Commun.* **239,** 357–366
47. Foti, M., Audhya, A., and Emr, S. D. (2001) *Mol. Cell. Biol.* **12,** 2396–2411
48. Warmka, J., Hanneman, J., Lee, J., Amin, D., and Ota, I. (2001) *Mol. Cell. Biol.* **21,** 51–60
49. Hageluken, A., Nurnberg, B., Harhammer, R., Grunbaum, L., Schunack, W., and Seifert, R. (1995) *Mol. Pharmacol.* **47,** 234–240
50. Honegger, U. E., Zuehlke, R. D., Scuntaro, I., Schaefer, M. H., Toplak, H., and Wiesmann, U. N. (1993) *Biochem. Pharmacol.* **45,** 349–356
51. Deziel, M. R., Davis, P. J., Davis, F. B., Cody, V., Galindo, J., Jr., and Blas, S. D. (1989) *Arch. Biochem. Biophys.* **274,** 463–470
52. Vig, P. J., Yallapragada, P. R., Kodavanti, P. R., and Desaiah, D. (1991) *Pharmacol. Toxicol.* **68,** 26–33
53. Vig, P. J., and Desaiah, D. (1991) *Neurotoxicology* **12,** 595–601
54. Roling, E. E., Klepser, M. E., Wasson, A., Lewis, R. E., Ernst, E. J., and Pfaller, M. A. (2002) *Diagn. Microbiol. Infect. Dis.* **43,** 13–17
55. Lupetti, A., Danesi, R., Campa, M., Del Tacca, M., and Kelly, S. (2002) *Trends Mol. Med.* **8,** 76–81
56. Kontoyiannis, D. P., Lewis, R. E., Sagar, N., May, G., Prince, R. A., and Rolston, K. V. (2000) *Antimicrob. Agents. Chemother.* **44,** 2915–2918